

1 **Production of peroxy nitrates in boreal biomass burning plumes over**
2 **Canada during the BORTAS campaign**

3

4 **Marcella Busilacchio¹, Piero Di Carlo^{1,2}, Eleonora Aruffo^{1,2}, Fabio Biancofiore^{1,2}, Cesare Dari**
5 **Salisburgo¹, Franco Giammaria², Stephane Bauguitte³, James Lee⁴, Sarah Moller⁴, James**
6 **Hopkins⁴, Shalini Punjabi⁴, Stephen Andrews⁴, Alistair C. Lewis⁴, Mark Parrington^{5,*}, Paul I.**
7 **Palmer⁵, Edward Hyer⁶, Glenn M. Wolfe^{7,8}**

8

9 [1] Center of Excellence CETEMPS, Universita' dell'Aquila, Via Vetoio, Coppito, L'Aquila, Italy,

10 [2] Department of Physical and Chemical Sciences, University of L'Aquila, Coppito L'Aquila, Italy,

11 [3] Facility for Airborne Atmospheric Measurements, Bedfordshire, UK,

12 [4] Department of Chemistry, University of York, York, UK,

13 [5] School of GeoSciences, University of Edinburgh, UK.

14 [6] Marine Meteorology Division, Naval Research Laboratory, Monterey, California, USA.

15 [7] Atmospheric Chemistry and Dynamics Laboratory, NASA Goddard Space Flight Center, Greenbelt,

16 Maryland, USA

17 [8] Joint Center for Earth Systems Technology, University of Maryland Baltimore County, Baltimore, MD,

18 USA

19 [*] now at European Centre for Medium-Range Weather Forecasts (ECMWF), Reading, UK.

20

21 Correspondence to: P. Di Carlo (piero.dicarlo@aquila.infn.it)

22

23

24 **Abstract**

25

26 The observations collected during the BORTAS campaign in summer 2011 over Canada are
27 analysed to study the impact of forest fire emissions on the formation of ozone (O₃) and total
28 peroxy nitrates (Σ PNs, Σ ROONO₂). The suite of measurements onboard the BAe-146 aircraft,
29 deployed in this campaign, allows us to calculate the production of O₃ and of Σ PNs, a long lived

1 NO_x reservoir whose concentration is supposed to be impacted by biomass burning emissions. In
2 fire plumes, profiles of carbon monoxide (CO), which is a well-established tracer of pyrogenic
3 emission, show concentration enhancements that are in strong correspondence with a significant
4 increase of ΣPNs concentrations, whereas minimal increase of the concentrations of O₃ and NO₂ are
5 observed. The ΣPNs and O₃ productions have been calculated using the rate constants of the first
6 and second order reactions of Volatile Organic Compounds (VOCs) oxidation. The ΣPNs and O₃
7 productions have also been quantified by 0-D model simulation based on the Master Chemical
8 Mechanism. Both methods show that in fire plumes the average production of ΣPNs and O₃ are
9 greater than in the background plumes, but the increase of ΣPNs production is more pronounced
10 than the O₃ production. The average ΣPNs production in fires plumes is from 7 to 12 times greater
11 than in the background, whereas the average O₃ production in fires plumes is from 2 to 5 times
12 greater than in the background. These results suggest that, at least for boreal forest fires and for the
13 measurements recorded during the BORTAS campaign, fire emissions impact both the oxidized
14 NO_y and O₃, but: 1) ΣPNs production is amplified significantly more than O₃ production and 2) in
15 the forest fire plumes the ratio between the O₃ production and the ΣPNs production is lower than the
16 ratio evaluated in the background air masses, thus confirming that the role played by the ΣPNs
17 produced during biomass burning is significant in the O₃ budget. The implication of these
18 observations is that fire emissions in some cases, for example Boreal forest fires and in the
19 conditions reported here, may influence more long lived precursors of O₃ than short lived
20 pollutants, which in turn can be transported and eventually diluted in a wide area.

21

22 **1. Introduction**

23 Biomass burning emissions are an important atmospheric source of fine carbonaceous particles,
24 trace gases and aerosols that significantly affect the chemical composition of the atmosphere and
25 the radiation balance of the Earth-atmosphere system (Crutzen et al., 1979; Crutzen and Andreae,
26 1990; Andreae and Merlet, 2001; Bond et al., 2004; Langmann et al., 2009; Bowman et al., 2009).

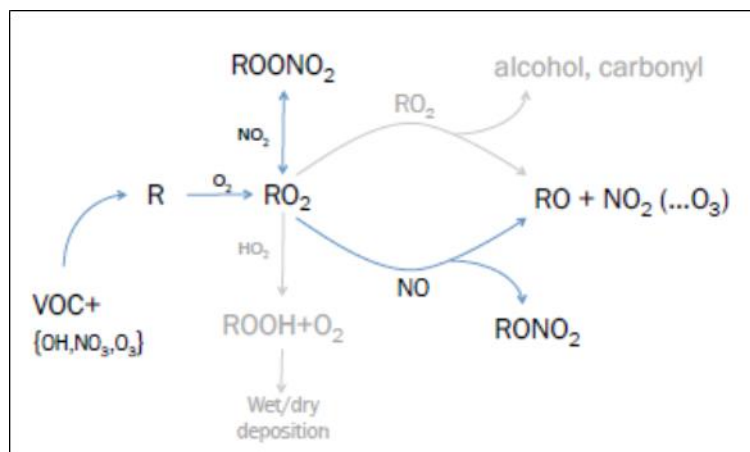
1 Biomass burning generates large quantities of carbon monoxide (CO), nitrogen oxides (NO_x=
2 NO+NO₂) and VOCs which are the major precursors involved in the photochemical production of
3 tropospheric ozone (O₃) (Goode et al., 2000, Chan et al., 2003). Moreover, biomass burning
4 emissions include some greenhouse gases (CO₂, CH₄, N₂O) that alter the climate and air quality
5 (Langmann et al., 2009; Lapina et al., 2006; Simpson et al., 2006). Quantification of the influence
6 of boreal forest fires on the Earth-atmosphere system and on the climate has become one of the key
7 topics for the scientific community.

8 Forest fires in the boreal regions of Siberia, Canada and Alaska peak during the period from May to
9 October (Lavoue et al., 2000). Some studies highlight the increase in the number of boreal forest
10 fires and the total forested area burned over Canada during the past three decades, corresponding to
11 increasing temperatures and reduced moisture in this area (Gillett et al., 2004; Rinsland 2007;
12 Marlon 2008). Wotton et al. (2010) estimate an increase of 30% in boreal forest fire occurrence by
13 2030, causing a possible growth of 30% in the emission of CO₂ and other greenhouse gases (Amiro
14 et al., 2009). The effects of boreal biomass burning emissions on the O₃ concentration has been
15 investigated by several authors with some studies showing situations where O₃ concentrations
16 increase and others where it was unaffected (e.g., Wofsy et al., 1992; Jacob et al., 1992; Mauzerall
17 et al., 1996; Wotawa and Trainer, 2000; Val Martin et al., 2006; Real et al., 2007; Leung et al.,
18 2007, Jaffe and Wigder, 2012, Parrington et al., 2012). The analysis of the ARCTAS-B (NASA
19 Arctic Research of the Composition of the Troposphere from Aircraft and Satellites) aircraft
20 measurements of biomass burning plumes in central Canada in the spring and summer of 2008
21 showed consistent production of peroxyacetyl nitrate (PAN), with little evidence for O₃ formation
22 and, in some plumes, the O₃ mixing ratios measured within boreal biomass burning plumes were
23 indistinguishable from measurements outside of the plumes (Alvarado et al., 2010). The production
24 of ozone $P(O_3)$ measured in boreal fire plumes has been reported to be a function of the plume age
25 (Parrington et al., 2013), but with mixed, non-conclusive results. For example, boreal fire plumes
26 transported over the Azores and measured between 1 and 2 weeks after emission showed an O₃

1 increase between 40% and 90% (Val Martin et al., 2006; Pfister et al., 2006). On the other hand,
2 observations over Siberia in 2006 of aged boreal fire plumes (up to a week) showed some plumes
3 with O₃ enhanced and others with O₃ depletion; on average, the O₃ in the fire plumes was not
4 significantly different from that in the background atmosphere (Verma et al., 2009). In earlier
5 studies of relatively fresh plumes (1-2 days), O₃ was reported to be enhanced in one third of the
6 boreal fire plumes with concentrations in the remaining plumes being unaffected (Wofsy et al.
7 1992; Mauzerall et al. 1996).

8 In the atmosphere, volatile organic compounds (VOCs) are oxidized by OH, NO₃ or O₃ producing
9 an alkyl radical R that rapidly reacts with molecular oxygen O₂ to form peroxy radicals (HO₂, RO₂)
10 (reaction R1). The RO₂, then, can proceed in different ways: 1) reacting with NO and producing a
11 molecule of alkyl nitrate (ΣANs, ΣRONO₂) (R2) or an alkoxy radical RO (R4) or 2) reacting with
12 NO₂ and producing peroxy nitrates (ΣPNs, ΣROONO₂) (R3). Reactions (R4) and (R3) have
13 opposite effects on the O₃ budget, propagating or terminating radical cycles, respectively. Thus,
14 peroxy nitrate formation competes with the O₃ production resulting from reactions (R4)-(R8). Alkyl
15 nitrate formation via (R2) can also affect the O₃ budget. The reaction cycles that are of interest
16 when considering Nitrogen oxides (NO_x) and odd-hydrogen radicals (HO_x) (R1-R8) are illustrated
17 schematically in Figure 1 and listed below:





1

2 **Figure 1.** A schematic of the atmospheric chemical system (Atkinson and Arey, 2003; Palmer et al.
3 2013).

4

5 The removal processes for the Σ PNs could be: 1) thermal dissociation into NO_2 ; 2) UV photolysis;
6 3) reaction with OH and 4) deposition. Different investigations have been done about the PAN
7 (MPAN, PPN) loss in different environments; for example, Roberts et al. (1998) showed that in a
8 marine boundary layer the likely mechanism for the PAN loss is the deposition in seawater or on
9 aerosol surface. Moreover, Cleary et al. (2007) described the PAN loss processes by thermal
10 decomposition indicating that its lifetime vary between hours (for a $T > 287$ K, lower troposphere)
11 to months (for a $T < 263$ K, mid-high latitude and free troposphere). They measured total PNs and
12 in order to evaluate the contribution of each individual PN (PN_i) to the total PNs, observing that
13 individual PNs are in steady state with their aldehydes precursors and their loss is the thermal
14 decomposition into NO_2 and the subsequent reaction of the peroxy radical (PA) with the NO.

15 In July and August 2011, the BOREal forest fires on Tropospheric oxidants over the Atlantic using
16 Aircraft and Satellites (BORTAS) measurement campaign was carried out in order to quantify the
17 impact of boreal biomass burning on the composition and distribution of tropospheric oxidants. The
18 BORTAS project involved several international institutions with the support of the UK Facility for
19 Airborne Atmospheric Measurements (FAAM). The instruments were installed on board the FAAM
20 BAe146 research aircraft and the campaign was based at Halifax airport (Nova Scotia, Canada).

1 During the campaign, fifteen flights were carried out (nominally referenced as flights B618 to
2 B632) in Eastern Canada that were planned to maximize the probability of sampling air masses
3 produced from forest fires in Canada (Ontario) or the USA. More detailed information about the
4 BORTAS campaign objectives and preliminary results are presented by Palmer et al. (2013).
5 The primary aim of this study is to evaluate and understand the impact of the boreal fire emissions
6 during the BORTAS campaign on the formation of O₃ and ΣPNs within biomass burning plumes
7 Our sub-objectives include: (i) identification and classification of the plumes through the pyrogenic
8 species analysis; (ii) determination of the sources of the biomass burning plumes using back-
9 trajectories.; (iii) understand the role played by the ΣPNs produced during biomass burning in the
10 O₃ budget; (iv) the estimation of the balance between the production of ozone and the production of
11 ΣPNs in this specific environment.

12

13 **2. Instrumental**

14 A comprehensive description of the BORTAS experiment and of the overall instrumentations
15 involved can be found in Palmer et al. (2013). Here we will describe briefly only the measurements
16 included in this analysis. NO₂, ΣPNs and ΣANs were measured using the TD-LIF (Thermal
17 Dissociation – Laser Induced Fluorescence) instrument developed at the University of L’Aquila
18 (Italy) (Dari-Salisburgo et al., 2009; Di Carlo et al., 2013). Briefly, this technique permits direct
19 measurement of NO₂ molecules excited by laser radiation. The ΣPNs and ΣANs are measured after
20 thermal-dissociation into NO₂ by heating the air sample at 200°C and 400°C, respectively (Day et
21 al., 2002; Di Carlo et al., 2013). Nault et al. (2015) found that methyl peroxy nitrate (CH₃O₂NO₂),
22 which can be abundant in particular conditions (very low temperature, below 240K, typical of the
23 high atmosphere), may contribute interference to high altitude NO₂ measurements resulting from
24 thermal decomposition occurring in the sample intake system. This interference is a function of the
25 intake system temperature and increases from 280 K in which the interference is negligible up to
26 300 K in which it can be on the order of 10%. During all the BORTAS flights analysed in this

1 paper, the cabin temperature has been kept at about 280 K and, as a consequence, the impact on the
2 NO₂ of the CH₃O₂NO₂ dissociation is negligible. Moreover, this species is not expected to be
3 significant in our study, since the ambient temperatures of the air masses sampled during the period
4 in analysis range between 250 K and 280 K and the CH₃O₂NO₂ concentration is significant only for
5 temperatures lower than 240 K. The measurements of O₃ were carried out with an UV absorption
6 system Model 49C (Thermo environmental Corp.) (Wilson and Birks, 2006). CO was measured
7 using a VUV resonance/fluorescence system (Gerbig et al. (1999)). A chemiluminescence
8 instrument equipped with a photolytic converter was also used to measure NO and NO₂ (Lee et al.
9 2009; Reidmiller et al. 2010). VOC concentrations were measured by the University of York using
10 a WAS (Whole Air Sampling) system coupled to an offline GC-FID (Gas Chromatography with
11 Flame Ionization Detector) (Hopkins et al. 2003; Purvis et al. 2013) and by the University of East
12 Anglia using a PTR-MS (Murphy et al. 2010). Observed compounds and a complete list of the
13 instruments on board the BAe-146 aircraft during BORTAS campaign with accuracy and detection
14 limit are reported in Palmer et al. (2013).

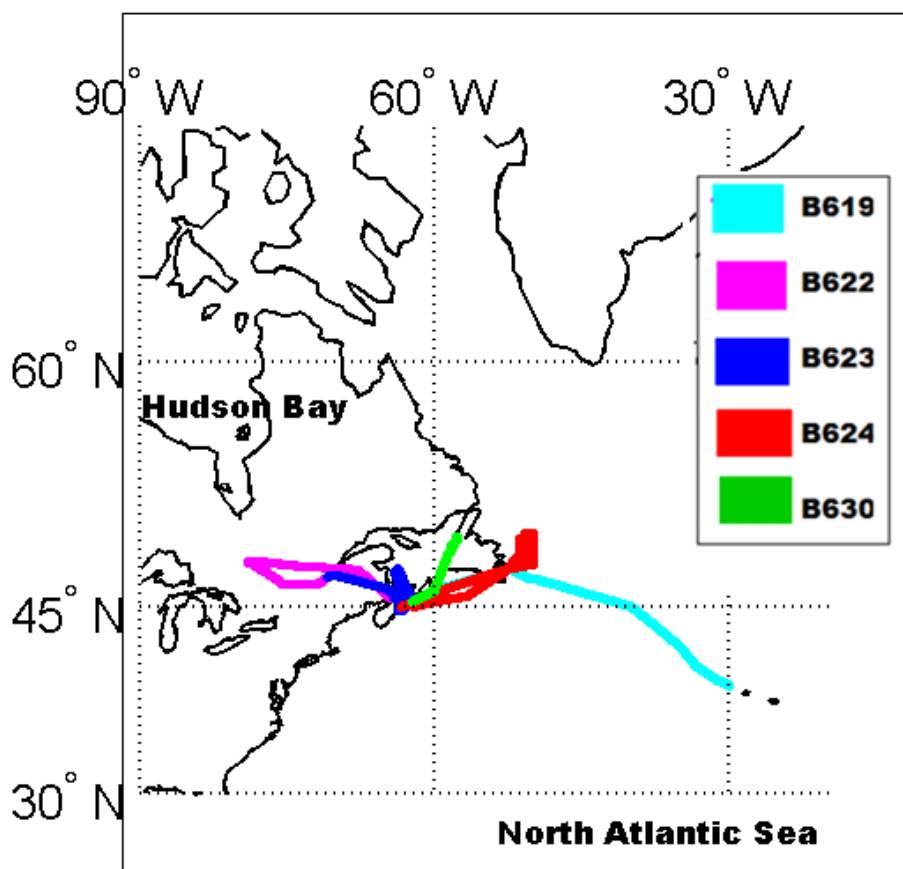
15

16 **3. Data analysis**

17 **3.1 Geographical location and meteorological situation**

18 Fig. 2 shows the geographic coverage of the five flights selected for our analysis. The flights were
19 carried out between 12th July and 3rd August 2011 over Canada and, in particular, above the North
20 Atlantic Ocean, Nova Scotia, Maine and Québec. The altitude during the flights exceeded a typical
21 planetary boundary layer depth of 2000 m a.s.l. so that local emissions do not affect the
22 measurements, especially those carried out in the fire plumes. The specific features of each flight
23 BORTAS and a description of the meteorology associated with them can be found in Palmer et al.
24 (2013). The synoptic situation of the fire plume flights analysed in this work, are similar to those of
25 background flights (Palmer et al., 2013).

26



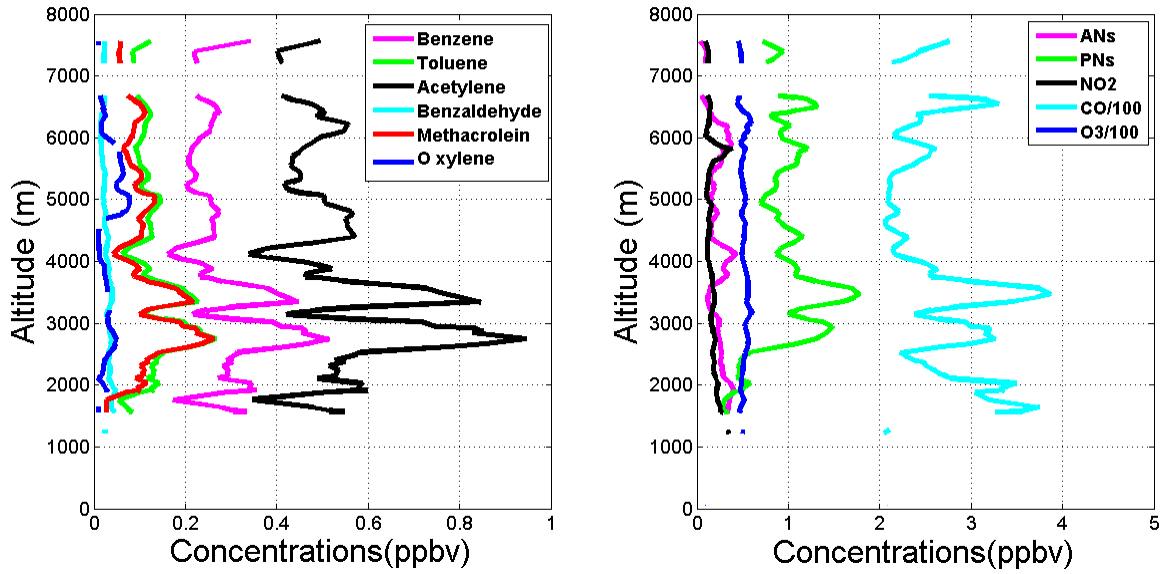
1
 2 **Figure 2.** FAAM146 flight tracks during July 2011. The different colours are the tracks of each
 3 different flight: during the B623 and B624 fire plumes were observed, during B619 and B630
 4 background air was measured, whereas in the B622 flight fire plume and background air were
 5 detected.

7 **3.2 Identification of the plumes: vertical profiles and back trajectories**

8 CO is a product of incomplete combustion (Crutzen et al., 1979; Andreae and Merlet, 2001; Lewis
 9 et al., 2013), therefore it is one of the tracers used to classify the plumes emitted by boreal fires.
 10 However, it is necessary to discriminate between anthropogenic and biomass burning CO
 11 emissions; for this purpose, following Lewis et al. (2013), we defined a CO threshold of 200 ppbv
 12 and we verified at the same time the presence of other pyrogenics such as furfural or camphor to
 13 confirm the fire origin of the plume. In conclusion, we classify the air masses in three classes: 1)
 14 those sampled within boreal biomass burning plumes ($\text{CO} \geq 200$ ppbv with significant presence of

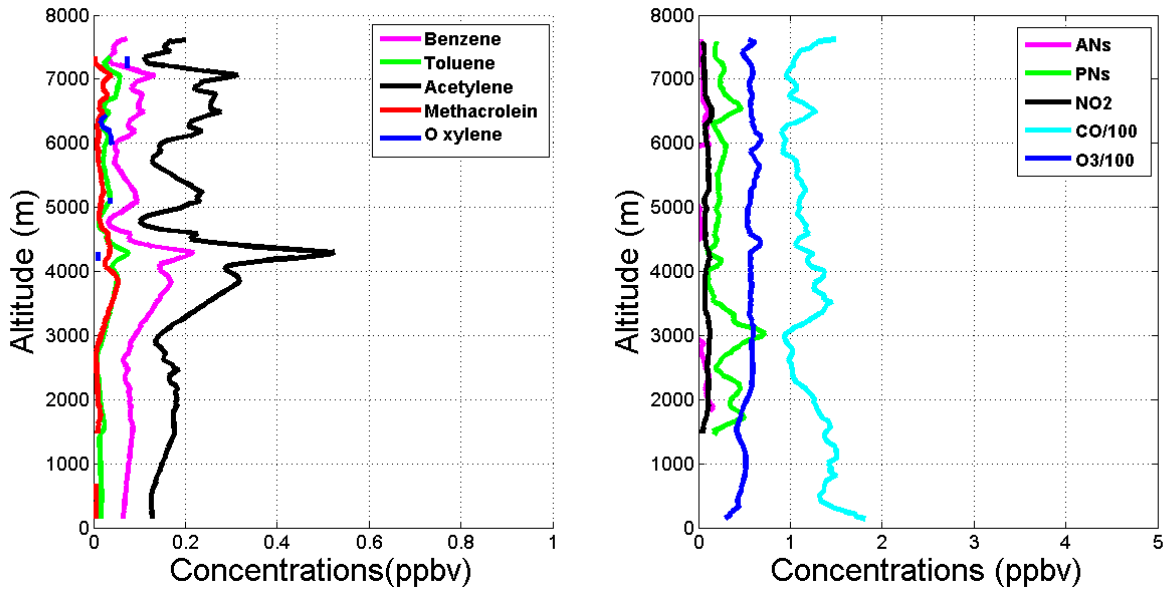
1 other pyrogenics species such as furfural or camphor (Andreae and Merlet, 2001); 2) those
2 impacted by anthropogenic emissions ($CO \geq 200$ ppb without the presence of furfural or camphor)
3 and 3) those sampled in background conditions ($CO < 200$ ppb). Using the above criteria to
4 distinguish between flights where we sampled fire plumes and those when we sampled background
5 air we analysed the vertical profiles of species known to have a significant biomass burning source,
6 such as NO_2 , ΣPNs , ΣANs , CO , O_3 and some $VOCs$ (i.e., propene, methacrolein, acetylene, benzene,
7 ethyl-benzene, toluene, o-xylene, benzaldehyde, furfural and camphor). The CO and pyrogenic
8 species analysis allows us to select five flights in which we distinguish between those where we
9 sampled boreal fire emissions (B622, B623 and B624 – labelled henceforth “plume” flights) and
10 those in which we measured background air (B619, B622 and B630 – labelled henceforth
11 “background” flights). Flight B622 is a particular case in which both conditions are met, and we
12 split this flight into two different parts: plume and background. Figure 3 shows profiles of the
13 species indicated above as a function of the altitude for the plume flights (upper panels) and for the
14 background flights (lower panels). It is possible to observe in Fig. 3 that the vertical structures are
15 different in the two conditions. In the upper panels (plume flights) the concentrations of some
16 species, especially CO , ΣPNs , Acetylene and Benzene, show significant and concomitant increases
17 at 3500 m above sea level (a.s.l.) and 6000 m a.s.l.. Moreover, in the plume measurements at 2000
18 m a.s.l. a large increase in the CO levels is measured concurrent with an increase in the ΣPNs
19 smaller than at the other altitudes. This suggests that the conditions of the air masses at 2000 m
20 a.s.l. are more complex and that it potentially has various origins, i.e., impacted both by
21 anthropogenic and boreal biomass burning emissions. The ΣANs concentrations are lower than the
22 ΣPNs and do not show significant structures. The O_3 profile shows little variability between 1000
23 and 7000 m of altitude with no concentration changes that coincide with variations in CO . In the
24 background flights, as expected, the concentrations of the species analysed do not show strong
25 vertical structures such as in the plume flights, with the exception of $VOCs$ that show a peak at
26 about 4 Km

FIRE PLUME



1

BACKGROUND



2

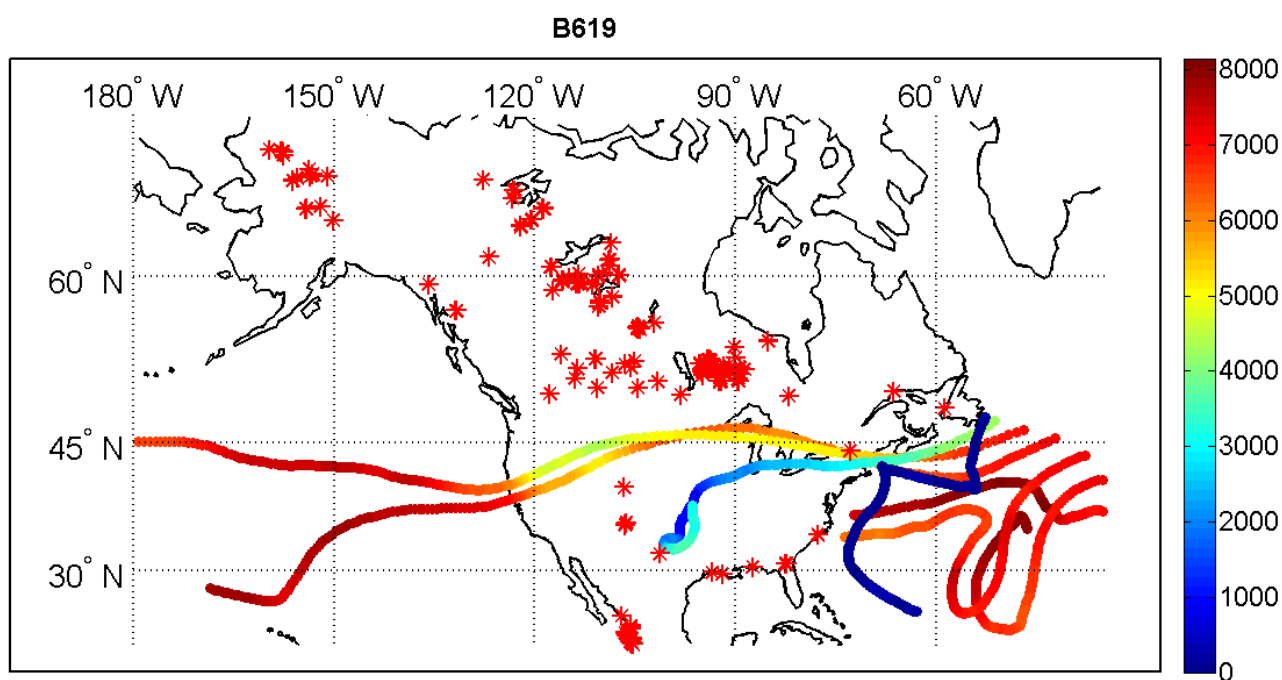
3 **Figure 3.** Vertical profiles of Benzene, Toluene, Acetylene, Methacrolein O-Xylene (panels on the
 4 left) and Σ ANs, Σ PNs, NO₂, CO and O₃ (panels on the right) concentrations averaged for the plume
 5 flights (upper panels: B622, B623, B624 flights) and the background flights (lower panels: B619,
 6 B622, B630 flights).

7

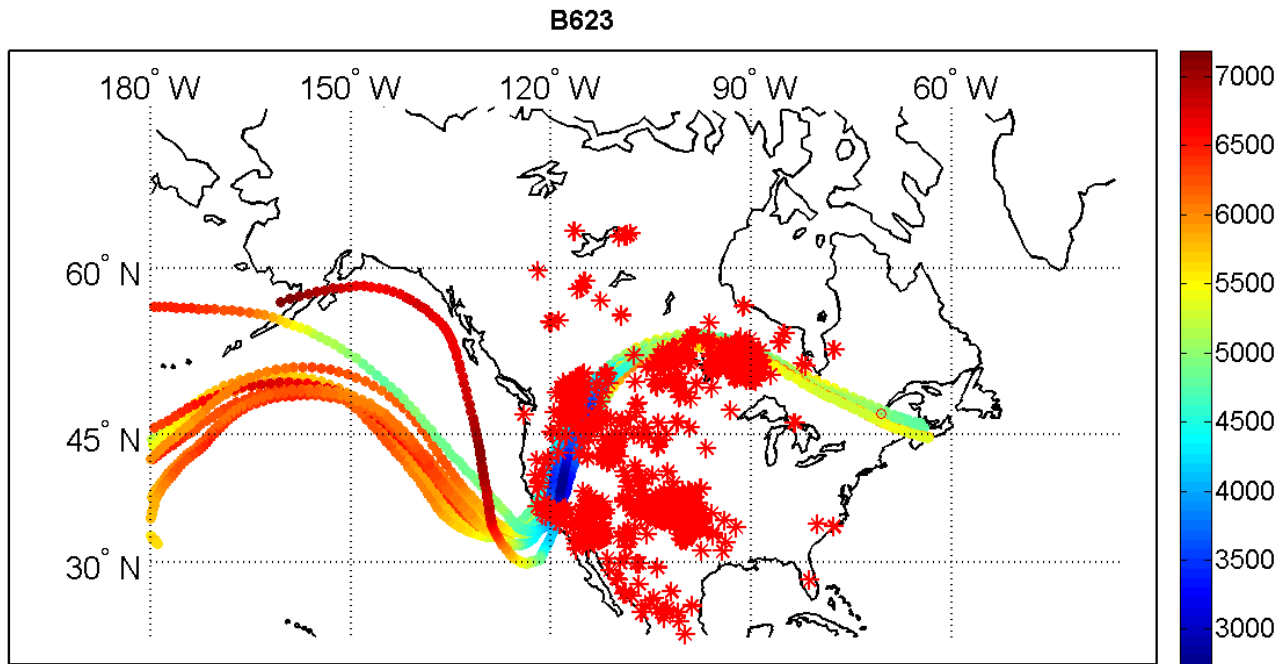
8 To facilitate the determination of the sources of the biomass burning plumes (Tereszczuk et al.,
 9 2011; Parrington et al., 2012), we calculated Lagrangian back trajectories using the Hysplit model
 10 (Draxler et al., 2003) to verify the origin of the air masses. The Fire Locating And Monitoring of

1 Burning Emissions (FLAMBE) archive provides fires emissions data from 2000 to the present
2 worldwide (Reid et al., 2009) incorporating active fire detection data from geostationary and polar-
3 orbiting satellites. To locate the sources of the boreal biomass burning plumes measured during the
4 BORTAS campaign, the FLAMBE inventory data have been used in conjunction with the Hysplit
5 back trajectories. In Fig. 4, 8 day back-trajectories are evaluated starting from points along the flight
6 track and the corresponding fires (red asterisks) from the FLAMBE archive are shown for the
7 plume flight B619 (upper panel) and for the background flight B623 (lower panel). The same
8 analysis has been done for all the flights of the campaign, although here we report only the results
9 of flights B619 and B623 since they are representative of all the other flights. Parrington et al.
10 (2013) evaluated the photochemical age of the air masses for each flight using the ratio of $\log(n-$
11 $butane/ethane)$ and assuming an OH concentration of 2×10^6 molecules/cm³. They found that the
12 age calculated for the air masses sampled within the boreal biomass burning emissions ranges
13 between 1 and 5 days and the background air is older than 6 days.

14
15
16



17



1

2 **Figure 4.** Location of the boreal biomass burning activity during the BORTAS campaign recorded
 3 by the FLAMBE inventory (red asterisks) and air mass backward trajectory analysis starting from
 4 location along the flight trajectories. The flight B623 (lower panel) sampled multiple fire plumes,
 5 whereas the flight B619 (upper panel) was representative of background conditions.

6

7 Their results are in agreement with the back-trajectories analysis, confirming that the air masses
 8 sampled during the plume flights crossed biomass fires during the previous 8 days and, conversely,
 9 the background air masses do not overlap fires up to 8 days before. In addition, Griffin et al.(2013)
 10 investigates boreal fire plumes during the BORTAS campaign using back trajectories calculated by
 11 the Canadian Meteorological Centre (CMC) and shows that the boreal fire plume originated from
 12 forest fires is approximately 1.5 days old, which is in agreement with the age calculated for the air
 13 masses sampled within the boreal biomass burning emissions.

14

15 3.3 Chemical signatures of plumes

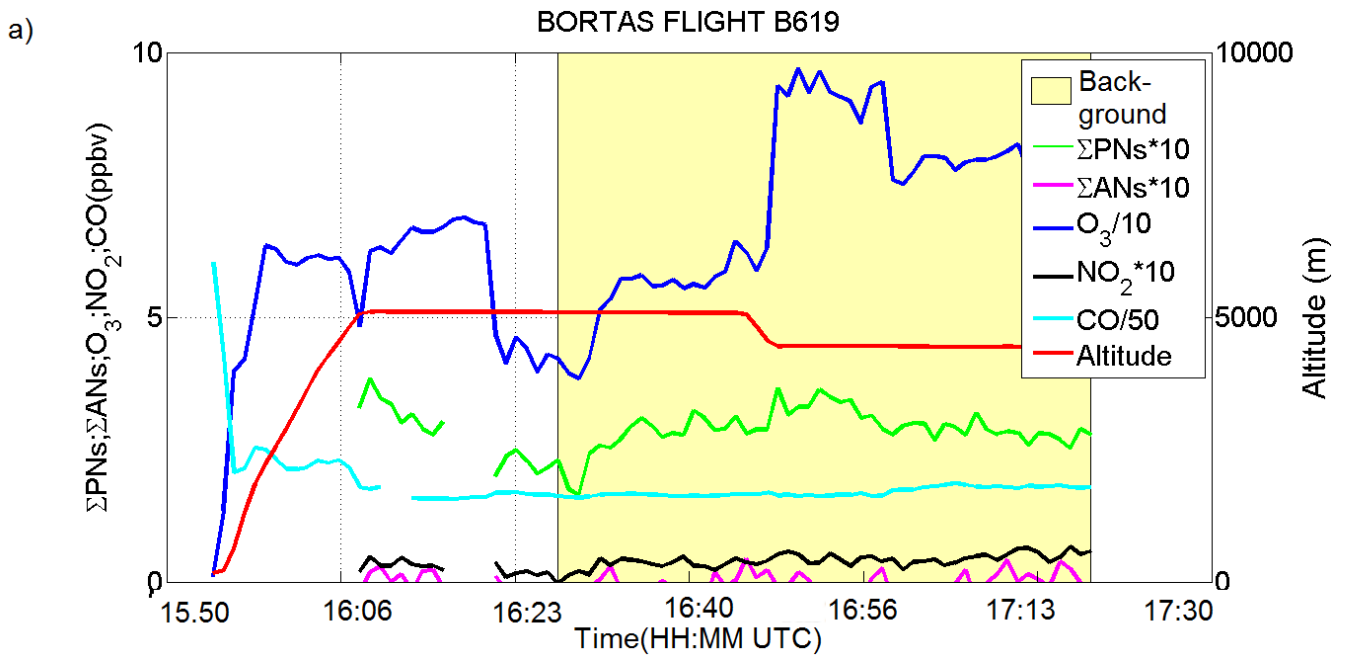
16 In Figure 5 the time series of NO₂, ΣPNs, ΣANs, O₃, CO and furfural (when measured) for the B619
 17 flight (panel a)) and the B630 flight (panel b)) are shown. During these background flights, the

1 concentrations of all the species measured remain quite stable. The Σ PNs concentrations are
2 significantly greater than the Σ ANs but lower compared to those measured in the plume flights (less
3 than 0.5 ppb). Moreover, Σ PNs do not show the significant structure that is shown in the O_3
4 measurements. CO is substantially lower than the 200 ppb threshold with the exception of one peak
5 measured during B619 during a period spent in the airport for refueling (at ground level) where the
6 CO level is affected by anthropogenic emissions and increases, reaching a maximum of about 300
7 ppb during take off.

8 The B622 flight (Fig. 5b) shows two regimes, as indicated by the CO concentrations and by the
9 furfural measurements. In the first part of the flight (between 2000 m a.s.l. and 4000 m a.s.l.,
10 highlighted by a grey box in Fig.5b) the CO levels (cyan line) exceed 150 ppb and the furfural
11 (yellow line) shows three big plumes (up to 1.2 ppb) in which the Σ PNs also increase (reaching the
12 maximum value of 3.5 ppb). On the other hand, in the second part of the flight the CO and Σ PNs
13 decrease and the furfural is below the detection limit indicating that the air sampled is not affected
14 by biomass burning. It is interesting to observe that O_3 and NO_2 concentrations are quite stable
15 flying within or outside of the fire plume. Flight B623 (Fig. 5c) represents a case in which the air
16 masses sampled for most of the flight were impacted by biomass burning emissions and the
17 remaining air masses show influence from human activities. In fact, CO levels are also always
18 greater than 200 ppb and the furfural is below the detection limit during the whole flight, indicating
19 an anthropogenic origin of the air masses. The fire plumes (highlighted by grey boxes) are
20 characterized by sharp increases in the CO concentrations (maximum value of 552 ppb) and in the
21 Σ PNs concentrations (maximum value of 1.5 ppb) measured while flying at constant altitude of
22 about 4000 m a.s.l.. In the final part of flight B623 (between 00:26 and 01:00 UTC) a vertical spiral
23 was carried out flying from 2000 m a.s.l. up to 8000 m a.s.l.. In this leg, plumes originating from
24 different fires (identified analyzing the Hysplit back trajectories) were sampled. At about 4000 m
25 a.s.l., back trajectories showed that the air masses sampled had the same origin of the fires plumes
26 sampled at the same altitude in the first part of the flight. Both plumes were characterized by high

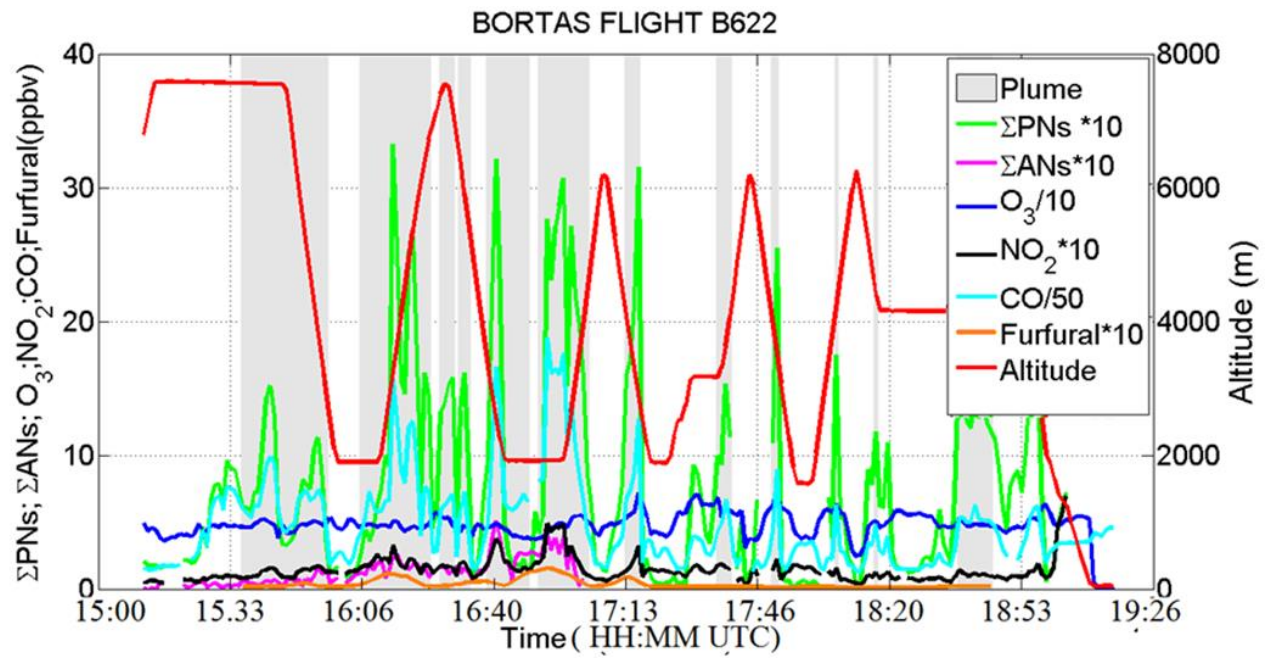
1 levels of Σ PNs (up to 1.7 ppb). At the top of the spiral (8000 m a.s.l.), an aged plume was
 2 encountered with low Σ PNs and O_3 concentrations quite high (about 60 ppb). This high O_3
 3 concentration represents the highest value measured during the whole flight.
 4 According to the back-trajectories, this air mass originated from fires in the Western States of the
 5 U.S.A. (Oregon, Montana, Washington, Idaho, California, Nevada).

6
7
8



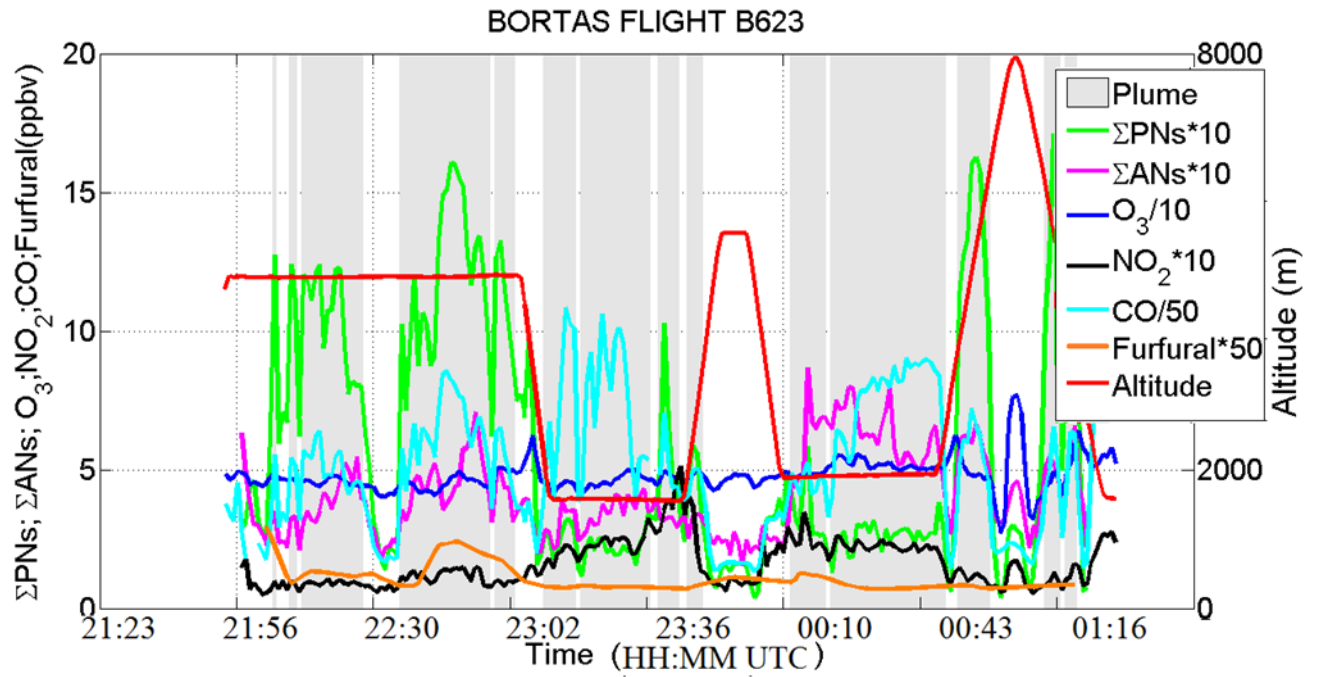
9
10

b)

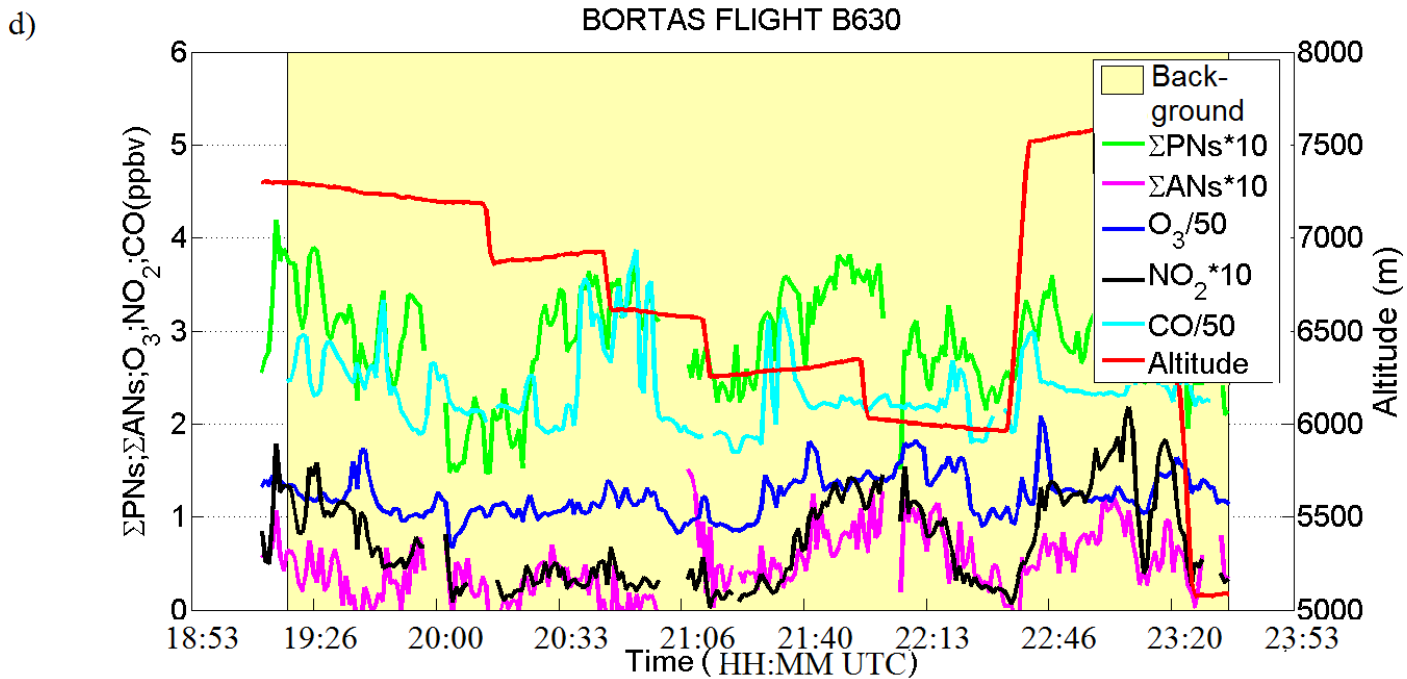


1
2

c)



3
4



2 **Figure 5.** Time series of the Σ PNs, Σ ANs, NO_2 , O_3 , CO, Furfural (ppbv) measured during the
 3 flights in this analysis: the flights B619 (panel a) and B630 (panel d) were background plumes, the
 4 flight B622 was in part impacted by fire plume and part by no-fire (panel b), the flight B623 (panel
 5 c) was affected by fire plume. The time is reported in Coordinated Universal Time (UTC).

6

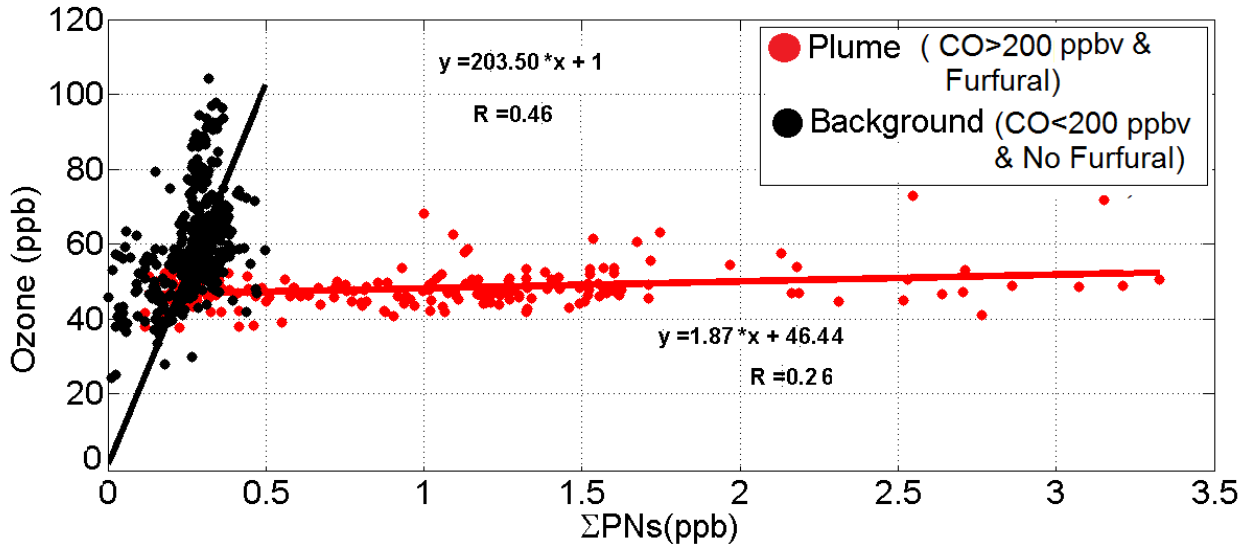
7

8 **3.4 Σ PNs and Ozone**

9

10 The connection between O_3 and Σ PNs is highlighted by the scatterplot of ozone vs Σ PNs mixing
 11 ratios in Fig. 6. Two different dependences can be identified distinguishing the air masses that are
 12 representative of the background environment (flights B619, part of the B622 and B630) and those
 13 emitted or influenced by emissions from biomass burning (flights B623, B624 and part of B622).
 14 We distinguished between the “plume” and the “background” flights as described in Sect. 3.2: that
 15 is based on the CO threshold ($\cong 200$ ppb) and the pyrogenic species analysis. The linear fit of the
 16 data influenced by biomass burning emissions has a slope of ~ 1.87 ppb O_3 /ppb Σ PNs compared to
 17 ~ 203.5 for the slope of the linear fit of background data, which indicates the important role played
 18 by the Σ PNs in the sequestration of ozone precursors in air masses influenced by fire emissions.

1 This can be quantified by calculating the productions of O₃ and ΣPNs, following the ΣANs
2 production schemes introduced by Atkinson (1985) and applied in other studies (Perring et al.
3 2010). This approach excludes the contribution of ANs for two reasons: 1) ANs concentrations are
4 very low in our observations strongly impacted by Bioreal biomass burning, so its contribution is
5 negligible; 2) to isolate the role of PNs from that of ANs in the O₃ that may dominate in particular
6 observations, like those reported here. We applied the same technique for the calculation of the PNs
7 production defining the branching ratio for the peroxy nitrates as $\alpha = k_{R3} / (k_{R3} + k_{R4})$. Therefore, the
8 ΣPNs production is given by $\alpha(\text{OH} + \text{RH} + \text{O}_2 + \text{NO}_2 \rightarrow \text{H}_2\text{O} + \text{RO}_2\text{NO}_2)$ and the O₃ production
9 is described as $(1 - \alpha)(\text{RH} + 4\text{O}_2 + h\nu \rightarrow \text{H}_2\text{O} + \text{R}'\text{C}(\text{O}) + 2\text{O}_3)$. In this description we made the
10 approximation of neglecting the impact of the [NO]/[NO₂] in the α calculation following Seinfeld
11 et al. (1997) that showed how the relative yield (α) of the PAN has a linear dependency on the ratio
12 between the NO and the NO₂. This is true for the [NO]/[NO₂] varying between 0 to 3.5 indicating
13 that the ratio between k_{R3} and k_{R4} is constant respect to this ratio. In our cases, [NO]/[NO₂] is
14 significantly lower than 3.5, therefore we can neglected the impact of [NO]/[NO₂] in the α
15 calculation. Moreover, they demonstrated that the ratio between k_{R3} and k_{R4} is independent from
16 the temperature and vary between ~0.04 and ~0.47 and our result, ~0.31 (see Table 1), is in
17 agreement with their observations.



1

2 **Figure 6.** Scatter plot between measured O₃ and measured ΣPNs for the flights B619, B622, B623,
 3 B624 and B630. Straight line is best fit linear regression. Plume identification follows the
 4 methodology and the analysis described in Sect. 3.2 and reported in the legend.

5

6

7 The production terms can be written as:

$$P(\sum \text{PNs}) = \sum_i \alpha_i k_{\text{OH}+\text{RH}_i} [\text{OH}] [\text{VOCs}] \quad (1)$$

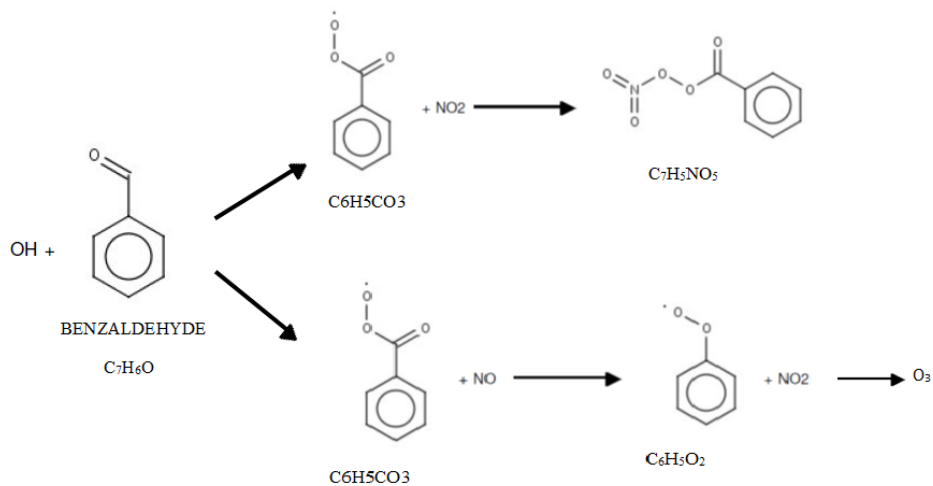
$$P(\text{O}_3) = \sum_i 2(1 - \alpha_i) k_{\text{OH}+\text{RH}_i} [\text{OH}] [\text{VOC}] + k_{\text{OH}+\text{CO}} [\text{OH}] [\text{CO}] \quad (2)$$

8

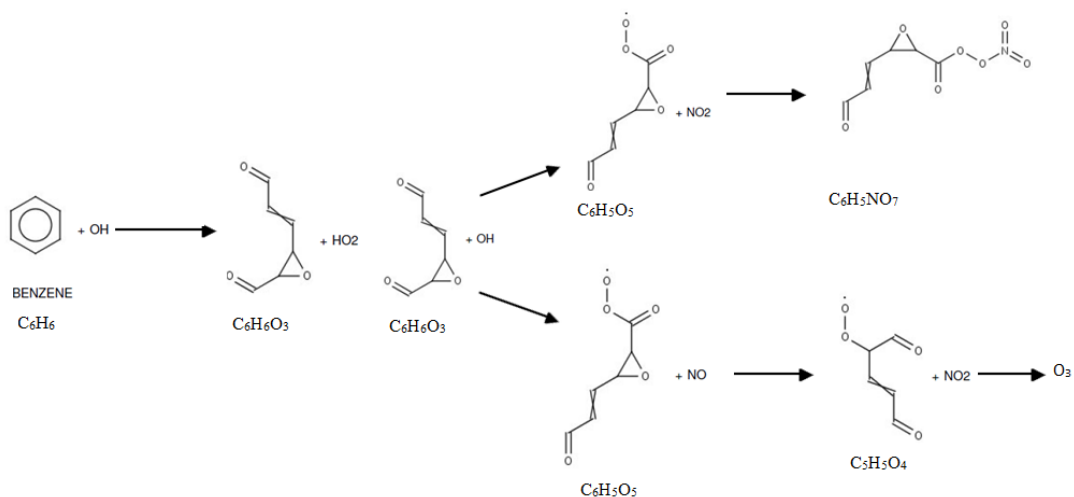
9 where we considered the weighted sum of the contribution of each VOC to the ΣPNs and to the O₃
 10 production. For the O₃ we take into account also the CO contribution on the $P(\text{O}_3)$ because of
 11 significant emissions associated with biomass burning.

12 In our analysis, we use two approaches to estimate the production of the ΣPNs and O₃: 1) a direct
 13 calculation considering the contribution to the PN_s and O₃ production of all the VOCs, among those
 14 measured during BORTAS, that produce a PN species after first or second order reactions of the
 15 VOCs oxidation by OH; in this case we considered only the production of ΣPNs and O₃ neglecting
 16 their losses; 2) a simulation using a box-model based on the Master Chemical Mechanism (MCM)

1 where all the measured VOCs are used as input compounds to evaluate in output the production of
2 PNs and O₃; in the model simulations we considered the net production of ΣPNs and O₃ (that is, the
3 production minus the loss). The mechanism used to calculate directly the ΣPNs and O₃ production
4 is similar for all the VOCs therefore we illustrate as an example the production mechanism of the
5 perbenzoyl nitrate (C₇H₅NO₅), derived from the first-order oxidation of the benzaldehyde (C₇H₆O)
6 (Figure 7, upper panel) and the production of the PN (C₆H₅NO₇), generated by the second-order
7 oxidation of the benzene (Figure 7, lower panel). In the first case, abstraction of the aldehydic
8 hydrogen by OH followed by O₂ addition forms an acyl peroxy radical (C₇H₅O₃). The acyl peroxy
9 radical can react either with NO₂ forming the perbenzoyl nitrate or with NO producing C₆H₅O₂ and
10 NO₂ (Figure 7, upper panel). In the second case, the production of PN starts with the benzene
11 oxidation by OH forming three different products: 11.8% of these reactions generate benzene-1,3,5-
12 triol (C₆H₆O₃) and HO₂. The benzene-1,3,5-triol oxidation by OH, in turn, produces a molecule of
13 C₆H₅O₅ in 31% of cases, that finally, reacts with NO₂ to form the peroxy nitrate C₆H₅NO₇ or with
14 NO generating C₅H₅O₄ plus NO₂ (Figure 7, lower panel). For the branch of benzene oxidation that
15 produces PN it is necessary to weight the contribution of the VOC oxidation to the PN formation by
16 applying a branching ratio of 0.118 to the reaction constant for the initial benzene oxidation by OH
17 and of 0.31 for the following benzene-1,3,5-triol oxidation: hereinafter we indicate the OH reaction
18 constant weighted following this method as k^* . The same procedure has been applied also to the
19 other VOCs that do not directly produce peroxy nitrates. Table 1 summarizes all the species
20 involved in the evaluation of the ΣPNs and O₃ production during all the flights, indicating for each
21 of them the OH reaction constant k^* and the branching ratio calculated as $\alpha = k_{R3} / (k_{R3} + k_{R4})$.



1



2

3 **Figure 7.** Examples of oxidation schemes that are common to all the VOCs that have as products
 4 PNs and O₃. Upper panel: structural formula of the oxidation of benzaldehyde that produces directly
 5 perbenzoyl nitrate (C₇H₅NO₅) and O₃. Lower panel: structural formula of the oxidation of benzene
 6 that produce O₃ and indirectly the PN (C₆H₅NO₇).

7

8 **Table 1.** Species involved in the calculation of peroxy nitrate and ozone production, their weighted
 9 reaction constant with OH (k^* expressed in cm³s⁻¹, see the text on how it is calculated) and the
 10 ΣPNs branching ratio (α).

Species	k^*	α
Methacrolein	1.48×10^{-11}	0.2777
Acetylene	2.37×10^{-13}	0.3084
Benzene	4.16×10^{-14}	0.3084
Ethylbenzene	1.82×10^{-13}	0.3084
Toluene	1.97×10^{-13}	0.3084
O-Xylene	7.29×10^{-12}	0.3084
Benzaldehyde	1.36×10^{-11}	0.3084
CO	2.39×10^{-13}	0

1

2 The reaction constants were extracted from the MCM model data or the references therein, and
3 from this, the branching ratios ($\alpha = k_{R3} / (k_{R3} + k_{R4})$) were calculated. For the branching ratio of
4 Methacrolein, the value of k_{R4} is $(8.70 \times 10^{-12}) \exp(290/T)$, where T is the temperature, and k_{R3} was
5 evaluated following the MCM model procedure that takes into account the ambient pressure. For
6 the other species, the k_{R4} reaction constant is $(7.50 \times 10^{-12}) \exp(290/T)$, where T is the ambient
7 temperature, and k_{R3} was evaluated as for methacrolein.

8 The simulation to retrieve the production of Σ PNs and O_3 were carried out using a 0-D
9 Photochemical Box Model (UW Chemical Model, UWCM) that is based on the Master Chemical
10 Mechanism (MCM) version v3.2 (<http://mcm.leeds.ac.uk/MCM/>) into a MATLAB-based source
11 code (Wolfe and Thornton 2011). The MCM is a nearly-explicit reaction set including primary,
12 secondary and radical species and about 17000 reactions to tracks all oxidation processes and
13 products throughout the photochemical degradation of VOCs. The inorganic chemistry has been
14 also included in the simulations. The photolysis reactions constants have been estimated from the
15 TUV model (<http://cprm.acd.ucar.edu/Models/TUV/>). The model has been initialized using both the
16 meteorological parameters (T, P, RH and J-values) and the chemical concentrations of NO, NO₂,

1 OH (fixed at 2×10^6 molecules/cm³, as for the direct calculation), CO, O₃ and all the VOCs (see
 2 Table 2) measured during BORTAS campaign. As no OH measurements were made during the
 3 BORTAS campaign, its value was chosen to be representative of a northern mid-latitude
 4 summertime OH concentration (Spivakovsky et al., 2000). This assumption was validated by
 5 Parrington et al. (2013) carrying out several tests in order to compare the photochemical ages using
 6 different OH concentrations with the transport timescales from the emission source determined by
 7 back trajectory calculations. Table 2 summarizes the mean concentrations of the VOCs and other
 8 species used in the simulations, the Σ PNs and O₃ production and their ratio for each flight analysed.
 9 The species highlighted with one asterisk have been used also for the direct calculation of Σ PNs and
 10 O₃ production terms. The quantities highlighted with two asterisks are the production of PNs and O₃
 11 calculated directly, while those without asterisks are the Σ PNs and O₃ production retrieved from the
 12 model simulations.

13
 14 **Table 2.** Concentrations of each species involved in the Σ PNs and O₃ production (all reported in
 15 ppt), the production terms $P(O_3)$ and $P(\Sigma PNs)$ (expressed in ppt/s), their ratios $P(O_3)/P(\Sigma PNs)$
 16 for all the flights analysed. While all the species reported in this table are used for the MCM model
 17 calculation of $P(O_3)$ and $P(\Sigma PNs)$, those with * are species used for the direct calculation of the
 18 production using the product between reaction constants and concentrations of the single species.
 19 The Σ PNs and O₃ production quantified with the model simulation are signed in this table with **.
 20 The selected flights are distinguished between the flights where we sampled boreal fire emissions
 21 (part of B622, B623 and B624 – labelled “plume” flights) and those in which we measured
 22 background air (B619, part of B622 and B630 – labelled “background” flights).

	Parameters	B619	B622	B630	B622	B623	B624
1	Ethane	1094.0	1209.8	975.1	4705.0	2407.5	1919.6
2	Propane	225.0	270.4	186.0	1141.2	563.4	432.3

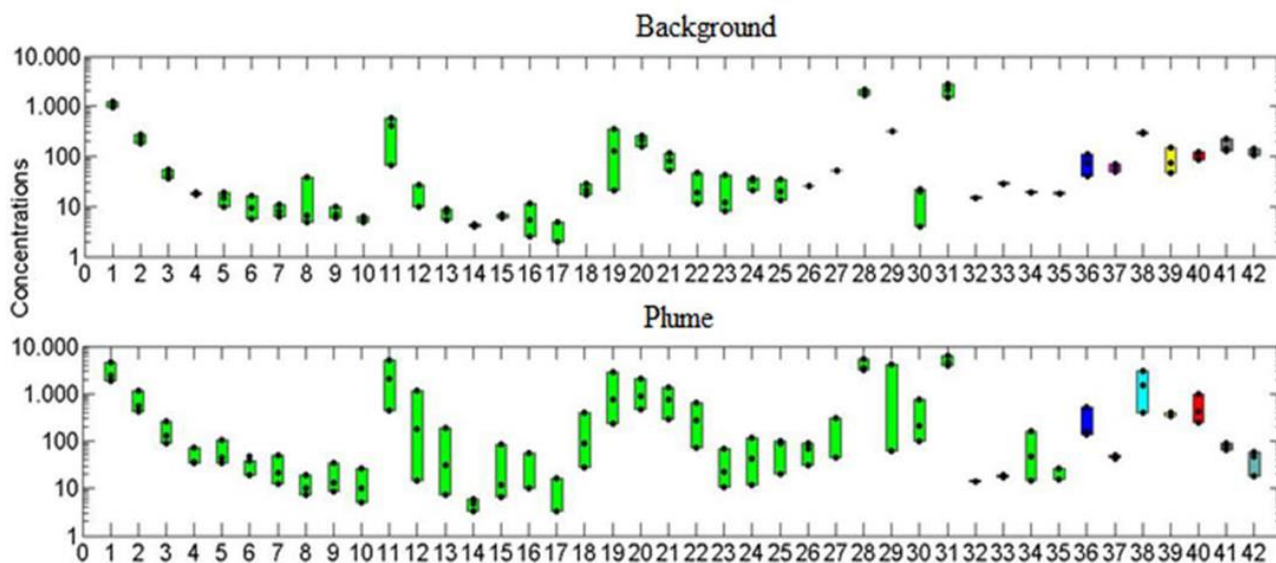
3	n-Butane	42.9	53.7	36.9	258.7	133.4	89.8
4	i-Butane	16.8	17.9	18.6	73.3	36.7	33.8
5	n-Pentane	14.5	18.7	10.1	106.2	46.1	34.7
6	i-Pentane	9.6	16.7	5.6	37.6	19.3	47.7
7	n-Hexane	11.0	8.0	6.3	49.4	21.0	12.7
8	2+3-Methylpentane	5.0	6.6	39.4	19.4	7.5	10.4
9	n-Heptane	6.0	9.9	6.8	35.1	13.5	8.8
10	n-Octane	4.8	5.4	6.2	26.0	10.3	5.1
11	Ethene	419.0	585.4	67.2	5115.2	2038.4	452.5
12	Propene	27.1	27.4	10.1	1127.6	179.8	14.7
13	1-Butene	7.7	9.1	5.3	185.0	31.4	7.3
14	Trans-2-butene	4.0	4.3	4.5	3.3	4.8	6.1
15	i-Butene	6.0	6.1	6.8	84.1	12.2	6.5
16	1-Pentene	5.3	11.4	2.6	56.7	10.0	-
17	Trans-2-pentene	2.0	4.8	4.9	16.1	3.4	-
18	1,3-Butadiene	28.3	17.1	21.4	399.1	88.9	27.5
19	Isoprene	20.5	347.5	130.4	2796.3	763.0	231.0
20	Acetylene *	256.3	208.8	156.6	2053.6	887.8	480.4
21	Benzene *	115.5	81.1	51.6	1387.0	776.0	291.4
22	Toluene *	46.4	18.7	11.6	636.2	282.0	72.6
23	O-Xylene *	12.3	7.9	43.2	68.6	22.5	10.8
24	m+p-Xylene	33.6	20.6	36.0	117.8	42.8	12.2
25	E-Benzene *	19.9	13.1	35.3	90.6	97.6	19.9
26	Benzaldehyde *	-	26.0	-	68.0	30.5	88.6
27	Acetophenone	-	51.8	-	44.0	46.2	312.3
28	Acetone	1692.1	1959.9	2144.8	5561.7	3166.5	3594.0
29	Methyl vinyl ketone	-	319.7	-	4126.0	-	62.2

30	Methacrolein *	22.5	20.4	4.0	754.5	213.3	100.6
31	Methanol	2119.0	2731.7	1549.9	6369.9	3950.8	4677.3
32	Limonene	-	15.0	-	14.3	-	14.3
33	α -Pinene	-	29.1	-	18.5	17.5	19.3
34	Furfural	-	19.4	-	157.5	46.5	14.4
35	Camphor	-	18.5	-	26.2	15.5	15.3
36	NO ₂	40.2	108.8	73.0	507.3	137.1	153.9
37	O ₃	71824.8	48217	61195	42431.0	45425	50858
38	Σ PNs (ppt)	288.5	281.9	298.2	2981.2	1543.2	407.8
39	Σ ANs (ppt)	148.9	72.3	46.9	404.8	399.8	335.0
40	CO (ppt)	84887.4	119559.0	119040	984590	419000	251540
	$P(O_3)$ (ppt/s) **	0.0420	0.0593	0.0581	0.5082	0.2120	0.1379
	$P(\Sigma PNs)$ (ppt/s)**	2.9719*	4.6631*	2.5807*	0.0078	0.0023	0.0017
		10 ⁻⁴	10 ⁻⁴	10 ⁻⁴			
41	$\frac{P(O_3)}{P(\Sigma PNs)}$ **	141.3	127.2	225.0	65.0	90.3	78.9
	$P(O_3)$ (ppt/s)	0.5133	1.8446	0.5554	5.5643	0.6263	0.2432
	$P(\Sigma PNs)$ (ppt/s)	0.0035	0.0163	0.0053	0.1182	0.0341	0.0041
42	$\frac{P(O_3)}{P(\Sigma PNs)}$	145.6	113.5	105.4	47.1	18.3	58.8

1

2

3



1

2

3 **Figure 8.** Average concentrations of the species involved in the O_3 and ΣPN_s production. VOCs are
 4 in green, CO in red, NO_2 in blue, O_3 in magenta, ΣPN_s in cyan and ΣAN_s in yellow. In grey is
 5 reported the ratio between the $P(O_3)$ and $P(\Sigma PN_s)$ evaluated using the direct calculation (see
 6 section 3.3); in teal blue is reported the ratio between the $P(O_3)$ and $P(\Sigma PN_s)$ evaluated using the
 7 model simulation. The upper shows data measured during background flights (B619, part of B622,
 8 B630); the lower panel shows data from fire plume flights (part of B622, B623, B624). The
 9 parameters showed in Figure 8 are numbered according to Table 2.

10

11 Figure 8 shows graphically the results summarized in Table 2. It is evident that during the
 12 background flights both the VOC and CO concentrations are significantly lower with respect to
 13 those measured during the plume flights, as expected. At the same time, however, the O_3 does not
 14 show significantly different concentrations in the biomass burning plumes. Conversely ΣPN_s
 15 concentrations in the fire plumes increase to a level three times higher than the measurements in
 16 background air masses and the alkyl nitrates double. Analysing the measured concentrations of O_3
 17 and ΣPN_s , we deduced that the boreal biomass burning emissions affect the ΣPN_s production more
 18 (on average 12 times higher in the fire plume compared with the background air) than the

1 production, which increase by only 5 times in the fire plume. Using the MCM simulation we got a
2 slightly different increase of Σ PNs production in the fire plume (on average 7 times), whereas the
3 O_3 production in the fire plume on average increases 2 times. Therefore in the fire plumes sampled
4 during the BORTAS campaign, with both methods we observed more production of NO_x reservoir
5 species, which can be transported and potentially impact the O_3 concentrations in other locations.
6 Alvarado et al. (2010), using a global chemical-transport model, estimated that 40% of the initial
7 NO_x emission from boreal forest fires were converted into PAN. Since PAN is one of the
8 compounds included in Σ PNs family, our results show that more production of Σ PNs in fire plumes
9 compared with background air is plausible. Moreover, calculating the ozone and peroxy nitrate
10 production ratio (Fig. 6), we found that it is lower in the fires plumes than in the background
11 samples. This suggests that the production of peroxy nitrates during the boreal biomass burning
12 becomes a significant process compared with the ozone production, at least in cold air when the
13 thermal dissociation of Σ PNs is not efficient. For example PAN, which is usually the most abundant
14 Σ PNs, has a lifetime strongly dependent on temperature: 1 hr at 300 K, 2 days at 273 K and 118
15 days at 250 K (Isaksen, 1985). In order to understand the impact of a specific category of VOCs, we
16 calculated the contribution of each VOC species and CO on the Σ PNs and O_3 production for the fire
17 plume flights (B622, B623 and B624). We find that the ozone production, as expected, is dominated
18 by CO (with percentages exceeding 93% for all the flights). Moreover, the production of peroxy
19 nitrates is dominated by methacrolein (with percentages ranging between 38% and 86%), followed
20 by benzaldehyde (47%-7%) and o-xylene (19%-3%). An unusual case, in terms of the peroxy
21 nitrates production, is the background flight (B630) during which 75% of $P(\sum PNs)$ is derived
22 from o-xylene and only 13% from methacrolein, which dominates on all the other flights analysed
23 in this study. At first look this is strange because methacrolein is one of the major products of
24 isoprene oxidation and it is expected that air masses coming from boreal forests (burning or not)
25 would be characterized by high concentrations of biogenic VOCs rather than o-xylene which is an

1 anthropogenic VOC. Lai et al. (2013) found that at the Taipei International Airport (Taiwan) the
2 most abundant VOCs produced by the aircraft exhaust emissions is o-xylene. During the B630
3 flight the altitude was of about 7000 m. a.s.l. (ranging between 7500-6000 m. a.s.l.), higher than the
4 other flights (1700-6000 m. a.s.l.), and the flight track was around the eastern coast of Canada:
5 Nova Scotia and Newfoundland Island. At the flight altitude of B630 it is possible to sample air
6 masses affected by aircraft emissions and, so it is likely that the o-xylene dominance on the Σ PNs
7 production can be explained due to emissions from aircraft traffic.

8 Finally, the analysis of the O_3 and Σ PNs production in different environments (background and
9 boreal biomass burning plumes) indicates the impact on the tropospheric O_3 budget of the fire
10 emissions. In fact, the air masses influenced by biomass burning emissions show a lower (about 90
11 with the direct method and about 40 with the model) $P(O_3)/P(\sum PNs)$ ratio with respect to that for
12 the background air masses (about 180 with the direct method and about 120 with the model)
13 suggesting that the ozone production in the fire plumes is less significant than the peroxy nitrate
14 formation, on the contrary of what occurs in the background air masses. The difference between the
15 calculate ratios and the measured O_3/Σ PNs (see Fig. 6) can be explained considering that: 1) the air
16 masses are not fresh emissions; 2) the Σ PNs production (term at the denominator) is
17 underestimated, as expected since we are not considering all the possible VOCs precursors but only
18 the available for the BORTAS campaign. Moreover, the higher VOCs and Σ PNs concentrations
19 measured during the fire plume flights, associated with stable O_3 levels in the two environments, are
20 indicative of processed air masses (produced 4-5 days before) and suggest that NO_2 reservoir
21 species are produced in these plumes and transported to other regions.

22

23 **4. Conclusions**

24

25 During the BORTAS aircraft campaign in Canada, we analysed the Σ PNs and O_3 production in two
26 different environments (air masses affected by fire emissions and those representative of

1 background air) using different approaches: 1) a direct calculation in which we considered the
2 VOCs oxidation rate constant and the Σ PNs branching ratios for all the VOCs species that produce
3 PN after the first or second order reaction of their oxidation by OH; 2) using a 0-D photochemical
4 model based on MCM that includes a detailed chemistry of all the VOCs measured. Comparing the
5 production of Σ PNs and O₃ in plumes impacted by fire emissions with that in background air, we
6 found that, on average, Σ PNs production is more strongly enhanced than O₃ production: 5 - 12 times
7 versus 2 - 7 times. Boreal biomass burning plumes observed during BORTAS campaign show
8 minimal enhancement of the O₃ and NO₂ concentrations and slight enhancement of the O₃
9 production. However, they show significant enhancement in both concentration and production of
10 Σ PNs, which can act as a reservoir and enhance ozone production downwind of the plume.

11

12 **Acknowledgments**

13 The BORTAS project was supported by the Natural Environment Research Council (NERC) under
14 grant number NE/F017391/1. M. Parrington was supported by the NERC grant. P. I. Palmer
15 acknowledges support from his Philip Leverhulme Prize.

16

17 **References**

- 18 Alvarado, M. J., J. A. Logan, J. Mao, E. Apel, D. Riemer, D. R. Blake, R. C. Cohen, K.-E. Min, A.
19 Perring, E. C. Browne, P. J. Wooldridge, G. S. Diskin, G. Sachse, H. Fuelberg, W. R. Sessions,
20 D. L. Harrigan, L. G. Huey, J. Liao, A. Case-Hanks, J. Jimenez-Palacios, M. J. Cubison, S. A.
21 Vay, A. Weinheimer, D. J. Knapp, D. D. Montzka, F. Flocke, I. B. Pollack, P. Wennberg, A.
22 Kurten, J. D. Crouse, J. M. St. Clair, A. Wisthaler, T. Mikoviny, R. M. Yantosca, C. C.
23 Carouge, and P. Le Sager :Nitrogen oxides and PAN in plumes from boreal fires during
24 ARCTAS-B and their impact on ozone: an integrated analysis of aircraft and satellite
25 observations, *Atmos. Chem. Phys.*, 10, 9739-9760, doi:10.5194/acp-10-9739-2010,2010.
- 26 Amiro, B. D., Cantin, A., Flannigan, M. D. and De Groot, W. J.: Future emissions from Canadian
27 boreal forest fires, *Canadian Journal of Forest Research*, 39(2), 383–395, doi:10.1139/X08-154,
28 2009.

1 Andreae, M. O. and Merlet, P.: Emission of trace gases and aerosols from biomass burning, *Global*
2 *Biogeochem. Cy.*, 15, 955–966, 2001.

3 Atkinson, R., Kinetics and Mechanisms of the Gas-Phase Reactions of the Hydroxyl Radical with
4 Organic Compounds under Atmospheric Conditions *Chem. Rev.* 85, 89-201, 1985.

5 Bowman, D.M.J.S., J.K. Balch, P. Artaxo, W.J. Bond, J.M. Carlson, M.A. Cochrane, C.M. D'Antonio,
6 R.S. DeFries, J.C. Doyle, S.P. Harrison, F.H. Johnston, J.E. Keeley, M.A. Krawchuk, C.A. Kull,
7 J.B. Marston, M.A. Moritz, I.C. Prentice, C.I. Roos, A.C. Scott, T.W. Swetnam, G.R. van der
8 Werf, and S.J. Pyne: Fire in the earth system, *Science*, 324, 481-484, 2009.

9 Chan, C. Y., Chan, L. Y., Harris, J. M., Oltmans, S. J., Blake, D. R., Qin, Y., Zheng, Y. G., and
10 Zheng, X. D.: Characteristics of biomass burning emission sources, transport, and chemical
11 speciation in enhanced springtime tropospheric ozone profile over Hong Kong, *J. Geophys. Res.*,
12 108, 4015, doi:10.1029/2001JD001555, 2003.

13 Chia-Hsiang Lai, Kuen-Yuan Chuang, Jin-Wei Chang: Source Apportionment of Volatile Organic
14 Compounds at an International Airport, *Aerosol and Air Quality Research*, 13: 689–698, 2013
15 Copyright © Taiwan Association for Aerosol Research ISSN: 1680-8584 print / 2071-1409
16 online doi: 10.4209/aaqr.2012.05.0121.

17 Cleary, P.A., Wooldridge, P.J., Millet, D.B., McKay, M., Goldstein, A.H., and, Cohen, R.C.,
18 Observations of total peroxy nitrates and aldehydes: measurement interpretation and inference of
19 OH radical concentrations, *Atmos. Chem. Phys*, 7, 1947-1960, 2007.

20 Crutzen, P.J., L.E. Heidt, J.P. Krasnec, W.H. Pollock and W. Seiler: Biomass burning as a source of
21 atmospheric gases CO, H₂, N₂O, NO, CH₃Cl and COS. *Nature*, 282, 253-256, 1979.

22 Dari-Salisburgo, C., Carlo, P. D., Giammaria, F., Kajii, Y., and D'Altorio, A.: Laser induced
23 fluorescence instrument for NO₂ measurements: Observations at a central Italy background
24 site, *Atmos. Environ.*, 43, 970–977, 2008.

25 Day, D. A., P. J. Wooldridge, M. B. Dillon, J. A. Thornton, and R. C. Cohen: A thermal
26 dissociation laser-induced fluorescence instrument for in-situ detection of NO₂, peroxy nitrates,
27 alkyl nitrates, and HNO₃, *J. Geophys. Res.*, 107(D6), 4046, doi:10.1029/2001JD000779, 2002.

28 Di Carlo, P., Aruffo, E., Busilacchio, M., Giammaria, F., Dari-Salisburgo, C., Biancofiore, F.,
29 Visconti, G., Lee, J., Moller, S., Reeves, C. E., Bauguitte, S., Forster, G., Jones, R. L., and
30 Ouyang, B.: Aircraft based four-channel thermal dissociation laser induced fluorescence
31 instrument for simultaneous measurements of NO₂, total peroxy nitrate, total alkyl nitrate, and
32 HNO₃, *Atmos. Meas. Tech.*, 6, 971–980, doi:10.5194/amt-6-971-2013, 2013.

33 Draxler, R. R.: HYSPLIT4 user's guide, Tech. Rep. NOAA Tech. Memo. ERL ARL-230, NOAA
34 Air Resources Laboratory, Silver Spring, MD, 1999.

1 Gerbig, C., S. Schmitgen, D. Kley, A. Volz-Thomas, K. Dewey, and D. Haaks: An improved fast-
2 response vacuum-UV resonance fluorescence CO instrument, *J. Geophys. Res.*, 104 (D1), 1699–
3 1704, 1999.

4 Gillett, N., A. J. Weaver, F. W. Zwiers, and M. D. Flannigan : Detecting the effect of climate
5 change on Canadian forest fires, *Geophys. Res. Lett.*, 31, L18211,
6 doi:10.1029/2004GL020876, 2004.

7 Goode, J. G., Yokelson, R. J., Ward, D. E., Susott, R. A., Babbitt, R. E., Davies, M. A., and Hao,
8 W. M.: Measurements of Excess O₃, CO₂, CO, CH₄, C₂H₄, C₂H₂, HCN, NO, NH₃, HCOOH,
9 CH₃COOH, HCHO and CH₃OH in 1997 Alaskan Biomass Burning Plumes by Airborne Fourier
10 Transform Infrared Spectroscopy (AFTIR), *J. Geophys. Res.*, 105, 22147–22166, 2000.

11 Griffin D., Walker K. A., Franklin J. E. , Parrington M., Whaley C. , Hopper J., Drummond J.
12 R., Palmer P. I. , Strong K., Duck T. J. , Abboud I., Bernath P. F., Clerbaux C. , Coheur P.F. ,
13 Curry K. R. , Dan L. , Hyer E. , Kliever J. , Lesins G., Maurice M., Saha A. , Tereszchuk K., and
14 Weaver D. Investigation of CO, C₂H₆ and aerosols in a boreal fire plume over eastern Canada
15 during BORTAS 2011 using ground- and satellite-based observations and model simulations
16 *Atmos. Chem. Phys.*, 13, 10227–10241, 2013

17 Hopkins, J. R., Read, K. A., and Lewis, A. C.: Two column method for long-term monitoring of
18 non-methane hydrocarbons (NMHCs) and oxygenated volatile organic compounds, *J.*
19 *Environ. Monitor.*, 5, 8–13, 2003.

20 Jacob, D. J., Wofsy, S. C., Bakwin, P. S., Fan, S.-M., Harriss, R.C., Talbot, R.W., Bradshaw, J.,
21 Sandholm, S., Singh, H. B., Gregory, G. L., Browell, E. V., Sachse, G. W., Blake, D. R., and
22 Fitzjarrald, D. R.: Summertime photochemistry at high northern latitudes, *J. Geophys. Res.*, 97,
23 16421–16431, 1992.

24 Jaffe, D.A., Wigder, N.L.: Ozone production from wildfires: A critical review. *Atmospheric*
25 *Environment* 51, 1–10, doi:10.1016/j.atmosenv.2011.11.063, 2012.

26 Jenkin, M. E., Saunders, S. M., Wagner, V., and Pilling, M. J.: Protocol for the development of the
27 Master Chemical Mechanism, MCM v3 (Part B): tropospheric degradation of aromatic volatile
28 organic compounds, *Atmos. Chem. Phys.*, 3, 181–193, doi:10.5194/acp-3-181-2003, 2003.

29 Isaksen, I. S. A., ed., *Tropospheric Ozone: Regional and Global Scale Interactions*, D. Reidel Pub.
30 Co., Dordrecht, NATO ASI Series C, Vol. 227, 1988.

31 Langmann, B., Duncan, B., Textor, C., Trentmann, J., and van der Werf, G. R.: Vegetation fire
32 emissions and their impact on air pollution and climate, *Atmos. Environ.*, 43, 107–116, 2009.

- 1 Lapina, K., Honrath, R.E., Owen, R.C., Val Martín, M., and Pfister, G.: Evidence of significant
2 large-scale impacts of boreal fires on ozone levels in the midlatitude Northern Hemisphere free
3 troposphere. *Geophys. Res. Lett.* 33, L10815, 2006.
- 4 Lavoué D, Lioussé C, Cachier H, Stocks BJ, Goldammer JG. :Modeling of carbonaceous particles
5 emitted by boreal and temperate wildfires at northern latitudes. *J. Geophys. Res.: Atmos.*
6 105(D22): 26871-26890,2000.
- 7 Lee, J. D., Moller, D. J., Read, K. A., Lewis, A. C., Mendes, L., and Carpenter, L. J.: Year-round
8 measurements of nitrogen oxides and ozone in the tropical North Atlantic marine boundary
9 layer, *J. Geophys. Res.*, 114, D21302, doi:10.1029/2009JD011878, 2009.
- 10 Leung, F.-Y. T., Logan, J. A., Park, R., Hyer, E., Kasischke, E., Streets, D., and Yurganov, L.:
11 Impacts of enhanced biomass burning in the boreal forests in 1998 on tropospheric chemistry
12 and the sensitivity of model results to the injection height of emissions, *J. Geophys. Res.*, 112,
13 D10313, doi:10.1029/2006JD008132, 2007.
- 14 Lewis, A. C., Evans, M. J., Hopkins, J. R., Punjabi, S., Read, K.A., Purvis, R. M., Andrews, S. J.,
15 Moller, S. J., Carpenter, L.J., Lee, J. D., Rickard, A. R., Palmer, P. I., and Parrington, M.:The
16 influence of biomass burning on the global distribution of selected non-methane organic
17 compounds, *Atmos. Chem. Phys.*, 13, 851–867, doi:10.5194/acp-13-851-2013, 2013.
- 18 Marlon, J. R., Bartlein, P. J., Carcaillet, C., Gavin, D. G., Harrison, S. P., Higuera, P. E., Joos,
19 F., Power, M. J., and Prentice, I. C.: Climate and human influences on global biomass burning
20 over the past two millennia, *Nature Geoscience* , 1, 69–702, 2008.
- 21 Mauzerall, D., Jacob, D. J., Fan, S.-M., Bradshaw, J., Gregory, G., Sachse, G., and Blake, D.:
22 Origin of tropospheric ozone at remote high northern latitudes in summer, *J. Geophys. Res.*,
23 101, 4175–4188, 1996.
- 24 Murphy, J. G., Oram, D. E., and Reeves, C. E.: Measurements of volatile organic compounds over
25 West Africa, *Atmos. Chem. Phys.*, 10, 5281–5294, doi: 10.5194/acp-10-5281-2010 , 2010.
- 26 Nault, B. A., Garland, C., Pusede, S. E., Wooldridge, P. J., Ullmann, K., Hall, S. R., Cohen, and R.
27 C.: Measurements of CH₃O₂NO₂ in the upper troposphere, *Atmos. Meas. Tech.*, 8, 987–997,
28 2015.
- 29 Palmer, P. I., Parrington, M., Lee, J. D., Lewis, A. C., Rickard, A.R., Bernath, P. F., Duck, T. J.,
30 Waugh, D. L., Tarasick, D. W., Andrews, S., Aruffo, E., Bailey, L. J., Barrett, E., Bauguitte, S.
31 J.-B., Curry, K. R., Di Carlo, P., Chisholm, L., Dan, L., Forster, G., Franklin, J. E., Gibson, M.
32 D., Griffin, D., Helmig, D., Hopkins, J. R., Hopper, J. T., Jenkin, M. E., Kindred, D., Kliever,
33 J., Le Breton, M., Matthiesen, S., Maurice, M., Moller, S., Moore, D. P., Oram, D. E., O’Shea, S.
34 J., Owen, R. C., Pagnliello, C.M. L. S., Pawson, S., Percival, C. J., Pierce, J. R., Punjabi,

1 S., Purvis, R. M., Remedios, J. J., Rotermund, K. M., Sakamoto, K. M., da Silva, A. M.,
2 Strawbridge, K. B., Strong, K., Taylor, J., Trigwell, R., Tereszchuk, K. A., Walker, K. A.,
3 Weaver, D., Whaley, C., and Young, J. C.: Quantifying the impact of BOREal forest fires on
4 Tropospheric oxidants over the Atlantic using Aircraft and Satellites (BORTAS) experiment:
5 design, execution and science overview, *Atmos. Chem. Phys.*, 13, 6239–6261, doi:10.5194/acp-
6 13-6239-2013, 2013.

7 Parrington, M., Palmer, P. I., Henze, D. K., Tarasick, D. W., Hyer, E. J., Owen, R. C., Helmig, D.,
8 Clerbaux, C., Bowman, K. W., Deeter, M. N., Barratt, E. M., Coheur, P.-F., Hurtmans, D., Jiang,
9 Z., George, M., and Worden, J. R.: The influence of boreal biomass burning emissions on the
10 distribution of tropospheric ozone over North America and the North Atlantic during
11 2010, *Atmos. Chem. Phys.*, 12, 2077–2098, doi:10.5194/acp-12-2077-2012, 2012.

12 Parrington, M., Palmer, P. I., Lewis, A. C., Lee, J. D., Rickard, A. R., Di Carlo, P., Taylor, J. W.,
13 Hopkins, J. R., Punjabi, S., Oram, D. E., Forster, G., Aruffo, E., Moller, S. J., Bauguitte, S. J.-
14 B., Allan, J. D., Coe, H., and Leigh, R. J.: Ozone photochemistry in boreal biomass burning
15 plumes, *Atmos. Chem. Phys.*, 13, 7321–7341, doi:10.5194/acp-13-7321-2013, 2013.

16 Pfister, G., Emmons, L. K., Hess, P. G., Honrath, R., Lamarque, J.-F., Val Martin, M., Owen, R. C.,
17 Avery, M., Browell, E. V., Holloway J. S., Nedelec, P., Purvis, R., Rywerson, T. B.,
18 Sachse, G. W., and Schlager, H.: Ozone production from the 2004 North American boreal fires, *J.*
19 *Geophys. Res.*, 111, D24S07, doi:10.1029/2006JD007695, 2006.

20 Perring A.E., Bertram T.H., Farmer D.K., Wooldridge P.J., Dibb J., Blake N.J., Blake D.R., Singh
21 H.B., Fuelberg H., Diskin G., Sachse G., and Cohen R.C. The production and persistence of
22 Σ RONO₂ in the Mexico City plume, *Atmos. Chem. Phys.*, 10, 7215–7229, 2010.

23 Purvis, R. M., Lewis, A. C., Hopkins, J. R., Andrews, S., and Minaean, J.: Functionalized aromatic
24 compounds within middle troposphere boreal biomass burning plumes, in preparation, 2013.

25 Real, E., Law, K. S., Weinzierl, B., Fiebig, M., Petzold, A., Wild, O., Methven, J., Arnold, S.,
26 Stohl, A., Huntrieser, H., Roiger, A., Schlager, H., Stewart, D., Avery, M., Sachse, G., Browell,
27 E., Ferrare, R., and Blake, D.: Processes influencing ozone levels in Alaskan forest fire plumes
28 during long-range transport over the North Atlantic, *J. Geophys. Res.*, 112,
29 D10S41, doi:10.1029/2006JD007576, 2007.

30 Reid, J. S., Hyer, E. J., Prins, E. M., Westphal, D. L., Zhang, J., Wang, J., Christopher, S. A., Curtis,
31 C. A., Schmidt, C. C., Eleuterio, D. P., Richardson, K. A., and Hoffman, J. P.: Global monitoring
32 and forecasting of biomass burning smoke: Description of and lessons from the Fire Locating
33 and Modeling of Burning Emissions (FLAMBE) program, *IEEE J. Sel. Top. Appl.*, 2, 144–162,
34 2009.

1 Reidmiller, D. R., Jaffe, D. A., Fischer, E. V., and Finley, B.: Nitrogen oxides in the boundary layer
2 and free troposphere at the Mt. Bachelor Observatory, *Atmos. Chem. Phys.*, 10, 6043–
3 6062, doi:10.5194/acp-10-6043-2010, 2010.

4 Rinsland, C. P., Dufour, G., Boone, C. D., Bernath, P. F., Chiou, L. Coheur, P.-F., Turquety, S., and
5 Clerbaux, C. :Satellite boreal measurements over Alaska and Canada during June–July 2004:
6 Simultaneous measurements of upper tropospheric CO, C₂H₆, HCN, CH₃Cl, CH₄, C₂H₂, CH₃OH,
7 HCOOH, OCS, and SF₆ mixing ratios, *Global Biogeochemical Cycles*, Vol.21,
8 GB3008, doi:10.1029/2006GB002795, 2007.

9 Roberts, J.M, Bertman, S.B., Parrish, D.D., and, Fehsenfeld, F. C., Measurement of alkyl nitrates at
10 Chebogue Point, Nova Scotia during the 1993 North Atlantic Regional Experiment (NARE)
11 intensive, *Journal of Geophysical Research*, 103, 13569-13580, 1998.

12 Saunders, S. M., Jenkin, M. E., Derwent, R. G., and Pilling, M. J.:WWW site of a master chemical
13 mechanism (MCM) for use in tropospheric chemistry models, *Atmos. Environ.*, (Report
14 Summary), 31, 1249, 1997.

15 Saunders, S. M., Jenkin, M. E., Derwent, R. G., and Pilling, M. J.: Protocol for the development of
16 the Master Chemical Mechanism, MCM v3 (Part A): tropospheric degradation of nonaromatic
17 volatile organic compounds, *Atmos. Chem. Phys.*, 3, 161–180, doi:10.5194/acp-3-161-2003,
18 2003.

19 Seefeld, S., David, J. K., and J., A. K., Relative Rate Study of the Reactions of Acetylperoxy
20 Radicals with NO and NO₂: Peroxyacetyl Nitrate Formation under Laboratory Conditions
21 Related to the Troposphere, *J. Phys. Chem. A*, 101, 55-59, 1997.

22 Simpson, I. J., Rowland, F. S., Meinardi, S., and Blake, D. R. :Influence of biomass burning during
23 recent fluctuations in the slow growth of global tropospheric methane, *Geophys. Res. Lett.*, 33,
24 L22808, doi:10.1029/2006GL027330, 2006.

25 Spivakovsky, C. M., Logan, J. A., Montzka, S. A., Balkanski, Y. J., Foreman-Fowler, M., Jones, D.
26 B. A., Horowitz, L. W., Fusco, A. C., Brenninkmeijer, C. A. M., Prather, M. J., Wofsy, S. C., and
27 McElroy, M. B.: Three-dimensional climatological distribution of tropospheric OH: Update and
28 evaluation, *J. Geophys. Res.*, 105, 8931–8980, 2000.

29 Tereszchuk, K. A., Gonz´alez Abad, G., Clerbaux, C., Hurtmans, D., Coheur, P.-F., and Bernath, P.
30 F.: ACE-FTS measurements of trace species in the characterization of biomass burning
31 plumes, *Atmos. Chem. Phys.*, 11, 12169–12179, doi:10.5194/acp-11-12169-2011, 2011.

32 Val Martin, M., Honrath, R., Owen, R. C., Pfister, G., Fialho, P., and Barata, F.: Significant
33 enhancements of nitrogen oxides, ozone and aerosol black carbon in the North Atlantic lower

- 1 free troposphere resulting from North American boreal wildfires, *J. Geo-phys. Res.*, 111,
2 D23S60, doi:10.1029/2006JD007530, 2006.
- 3 Verma, S., Worden, J., Pierce, B., Jones, DBA., Al-Saadi, J., Boersma, F., Bowman, K., Eldering,
4 A., Fisher, B., Jourdain, L., Kulawik, S., Worden, H. :Ozone production in boreal fire smoke
5 plumes using observations from the Tropospheric Emission Spectrometer and the Ozone
6 Monitoring Instrument, *J. Geophys. Res.*, 114, 0.1029/2008JD010108,2009.
- 7 Wilson, K. L. and J. W. Birks: Mechanism and Elimination of a Water Vapor Interference in the
8 Measurement of Ozone by UV Absorbance, *Environmental Science and Technology* 40, 6361-
9 6367,2006.
- 10 Wofsy, S.C., Sachse, G.W., Gregory, G.L., Blake, D.R., Bradshaw, J.D., Sandholm, S.T., Singh,
11 H.B., Barrick, J.A., Harriss, R.C., Talbot, R.W., Shipham, M.A., Browell, E.V., Jacob, D.J. and
12 Logan, J.A.:Atmospheric chemistry in the Arctic and subarctic: Influence of natural fires,
13 industrial emissions, and stratospheric inputs. *Journal of Geophysical Research*, 97: doi:
14 10.1029/92JD00622. issn: 0148-0227, 1992.
- 15 Wolfe, G.M. and Thornton, J.A.: The Chemistry of Atmosphere Forest Exchange (CAFE) Model -
16 Part 1:Model Description and Characterization, *Atmospheric Chemistry and Physics*, 11, 77-101,
17 2011.
- 18 Wotawa, G., and M. Trainer :The influence of Canadian forest fires on pollutant concentrations in
19 the United States. *Science* 288(5464):324-328,2000.
- 20 Wotton, B. M., Nock, C. A., and Flannigan, M. D.: Forest fire occurrence and climate change in
21 Canada, *International Journal of Wildland Fire*, 19, 253–271, 2010.